Biochimica et Biophysica Acta 1788 (2009) 500–506

Contents lists available at ScienceDirect

Biochimica et Biophysica Acta

journal homepage: www.elsevier.com/locate/bbamem

K^+ binding in the G-loop and water cavity facilitates Ba^{2+} movement in the Kir2.1 channel

Hsueh-Kai Chang [a], Laurence J. Marton [b], Kuo Kan Liang [c], Ru-Chi Shieh [a,*]

[a] Institute of Biomedical Sciences Academia Sinica 128 Yen-Chiu Yuan Road, section 2 Taipei 11529 Taiwan
[b] Progen Pharmaceuticals, Inc., Redwood City, CA 94065, USA
[c] Division of Mechanics, Research Center for Applied Sciences, Academia Sinica and Department of Biochemical Science and Technology, National Taiwan University, Taipei, Taiwan

ARTICLE INFO

Article history:
Received 23 July 2008
Received in revised form 12 October 2008
Accepted 21 October 2008
Available online 5 November 2008

Keywords:
Permeation
Selectivity filter
Channel block
Polyamines

ABSTRACT

K^+ are selectively coordinated in the selectivity filter and concerted K^+ and water movements in this region ensure high conduction rates in K^+ channels. In channels with long pores many K^+ binding sites are located intracellular to the selectivity filter (inner vestibule), but their contribution to permeation has not been well studied. We investigated this phenomenon by slowing the ion permeation process via blocking inwardly rectifying Kir2.1 channels with Ba^{2+} in the selectivity filter and observing the effect of K^+ in the inner vestibule on Ba^{2+} exit. The dose–response effect of the intracellular K^+ concentration ($[K^+]_i$) on Ba^{2+} exit was recorded with and without intracellular polyamines, which compete with K^+ for binding sites. Ba^{2+} exit was facilitated by the cooperative binding of at least three K^+. Site-directed mutagenesis studies suggest that K^+ interacting with Ba^{2+} bound in the selectivity filter were located in the region between selectivity filter and cytoplasmic pore, i.e. the water cavity and G-loop. One of the K^+ binding sites was located at residue D172 and another was possibly at M301. This study provides functional evidence for the three K^+ binding sites in the inner vestibule previously identified by crystal structure study.

1. Introduction

K^+ channels are multi-ion pores that selectively allow K^+ to bind with high affinity while allowing high conduction rates. How K^+ channels conduct K^+ selectively, yet at rates approaching the diffusion limit, has been attributed to the balance between ion channel affinity and ion–ion repulsion [1–5]. The crystal structures of K^+ channels have revealed several K^+ binding sites in the pore, with two K^+ binding sites located near the extracellular opening, four in the selectivity filter, and one in the water cavity [6,7]. Recently, in a chimeric channel formed by splicing Kir3.1 and KirBac1.3 channels, two other K^+ binding sites were identified at positions corresponding to the inner helix bundle gate (near M301 in the Kir2.1 channel) and the apex of the inner vestibule formed by the G-loop (near A306 in the Kir2.1 channel) [7]. MacKinnon et al. [6,8] have suggested that the four selectivity-filter sites are not all occupied simultaneously. Using ion-occupancy measurements, they further suggested that two K^+ separated by a single water molecule shift in a concerted fashion between two configurations within the filter until a third K^+ enters the selectivity filter, displacing the ion on the opposite end of the queue [6]. Since the energy difference between the two configurations is close to zero for K^+, the maximum conduction rate is achieved [6]. By carrying out molecular dynamics free energy simulations based on the structure of the KcsA K^+ channel, it has been suggested that ion conduction involves transitions between two states with either two or three K^+ in the selectivity filter and that the two K^+ binding states and the transition state are energetically similar [9]. In other words, the conduction process in the selectivity filter is energetically barrierless [9].

The importance of K^+ binding and concerted K^+ transport in the selectivity filter has been clearly demonstrated, but these properties have not been well studied in the pore intracellular to the selectivity filter (referred to as the "inner vestibule" in this study). Fig. 1 shows that the inner vestibule consists of the water cavity, the G-loop [10], and a wide cytoplasmic pore. Although the translocation of K^+ in single file through the selectivity filter is expected to be the rate-limiting step in ion permeation, the contributions of other parts of the channel to total conduction may also be important. In particular, although the inner vestibules of inward-rectifier K^+ channels are very long [7,11], the interaction of K^+ with each other and with the channel pore in this region has not been well studied. Since K^+ conduction is very fast (near the diffusion limit), it is difficult to determine the contribution of K^+ in the inner vestibule to ion permeation in K^+ channels. Our approach to investigating this topic was to slow down the ion permeation process by blocking Kir2.1 channels with Ba^{2+} [12]. It has previously been shown that a T141V mutation in the Kir2.1 channel decreases Ba^{2+} binding affinity in the pore, whereas a V140T (equivalent to T141 in the Kir2.1 channel) mutation in the Ba^{2+}-insensitive Kir1.1 channel increases Ba^{2+} affinity [13]. Furthermore, the crystal structure of the KcsA channel shows that Ba^{2+} is bound at, or

* Corresponding author. Tel.: +886 2 2652 3914; fax: +886 2 2782 9143.
E-mail address: ruchi@ibms.sinica.edu.tw (R.-C. Shieh).

0005-2736/$ – see front matter © 2008 Elsevier B.V. All rights reserved.
doi:10.1016/j.bbamem.2008.10.016

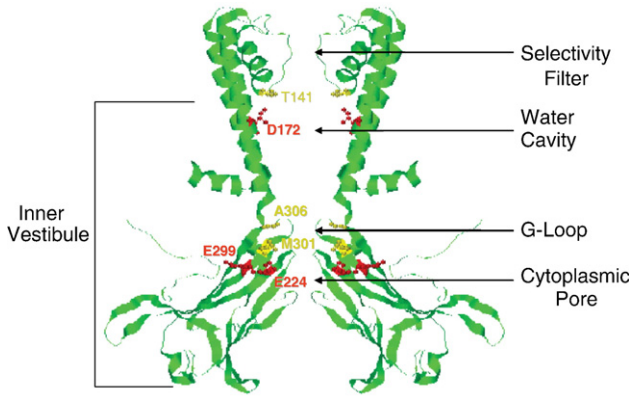

Fig. 1. Homology model of Kir2.1 channel structure. The model was constructed based on sequence alignment with the structure of a Kir3.1-prokaryotic chimera [7]. Two of the four subunits of the Kir2.1 channel are shown. Residues involved in K^+, Ba^{2+}, and spermine bindings are shown as ball-and-chain models.

near, a single location (equivalent to T141 in the Kir2.1 channel) [14]. Based on these findings, we assumed that Ba^{2+} is bound at, or near, the T141 site. We then studied the role of K^+ in the inner vestibule in the process of Ba^{2+} exit and found that the cooperative interaction of at least three K^+ in the G-loop and water cavity was required for Ba^{2+} exit to the extracellular side.

2. Materials and methods

2.1. Molecular biology and preparation of Xenopus oocytes

Mutations were constructed using PCR and checked by sequencing. cRNAs were obtained by in vitro transcription (mMessage mMachine, Ambion, Dallas, USA). *Xenopus* oocytes were isolated by partial ovariectomy from frogs anaesthetized with 0.1% tricaine (3-amino-benzoic acid ethyl ester). All surgical and anesthetic procedures were reviewed and approved by the Academia Sinica Institutional Animal Care and Utilization Committee. Oocytes were maintained at 18 °C in Barth's solution containing (in mM): NaCl (88), KCl (1), $NaHCO_3$ (2.4), CaN_2O_6 (0.3), $CaCl_2$ (0.41), $MgSO_4$ (0.82), HEPES (15), and gentamicin (20 μg/ml), pH 7.6, and were used for electrophysiology 1–3 days after cRNA injection.

2.2. Electrophysiology

Giant-patch recordings were sampled at 10 kHz and filtered at 2 kHz using the patch clamp technique [15,16] and an Axopatch 200B amplifier (Axon Instruments, Foster City, USA) at room temperature (21–24 °C). The extracellular solution contained (in mM): KCl (71), KOH (20), EDTA (5), K_2HPO_4 (4), and KH_2PO_4 (1), pH 7.4. The 30–600 mM $[K^+]_i$ intracellular solutions contained (in mM): KCl (1–571), KOH (20), EDTA (5), K_2HPO_4 (4), and KH_2PO_4 (1), pH 7.4; in the cases of the 30, 50, and 75 mM $[K^+]$ solutions, 140, 100, or 50 mM sucrose was added, respectively, to keep the viscosity constant. The 20 and 4 mM $[K^+]_i$ intracellular solutions contained respectively (in mM): KOH (11), EDTA (2), sucrose (160), K_2HPO_4 (4), and KH_2PO_4 (1), pH 7.4, and KOH (4), EDTA (0.5), sucrose (192), and HEPES (5), pH 7.4. The free $[Ba^{2+}]$ (3 μM) in the extracellular solution was calculated using the MaxC program (Chris Patton, Stanford University) and the stability constants reported by Martell and Smith [17].

The membrane voltage (V_m) was controlled, and data acquisition processed, using a personal computer, a DigiData board, and pClamp6 software (Axon Instruments, Foster City, CA, USA). CGC-11179 (~46 Å long), a synthetic polyamine with 10 amines, was synthesized and provided by Progen Pharmaceuticals, Inc. (Redwood City, California, USA).

2.3. Data analysis

Throughout the study, 3 μM $[Ba^{2+}]$ was used for Ba^{2+} block and recovery experiments. At this concentration, extracellular Ba^{2+} does not block the instantaneous inward currents through the Kir2.1 channel and the block process follows a first-order reaction [18]. Therefore, the Ba^{2+} exit rate (k_{off}) could be estimated from the time constant for recovery from Ba^{2+} block (τ_{recov}) and the association rate constant (k_{on}) using the equation:

$$k_{off} = 1/\tau_{recov} - k_{on} \times [Ba^{2+}] \quad (1)$$

Due to the low binding affinity of extracellular Ba^{2+} to the Kir2.1 channel at $V_m > -40$ mV (Fig. 2A), k_{on} could not be accurately determined at $V_m \geq 0$ mV. Therefore, we estimated k_{on} at V_m ranging from −150 to −50 mV and then obtained k_{on} values at $V_m \geq 0$ mV from extrapolation as follows.

We first calculated k_{on} as previously described [19] from the following equation:

$$k_{on} = (1-f)/(\tau_{block} \times [Ba^{2+}]) \quad (2)$$

where $f = I_{ss}/I_{inst}$, is the steady-state channel block by Ba^{2+}. I_{ss} and I_{inst} are the steady state and instantaneous currents. τ_{block} is the time constant for the decay of inward currents induced by extracellular Ba^{2+} and is obtained by exponential fit to inward currents. Fig. 2A shows that

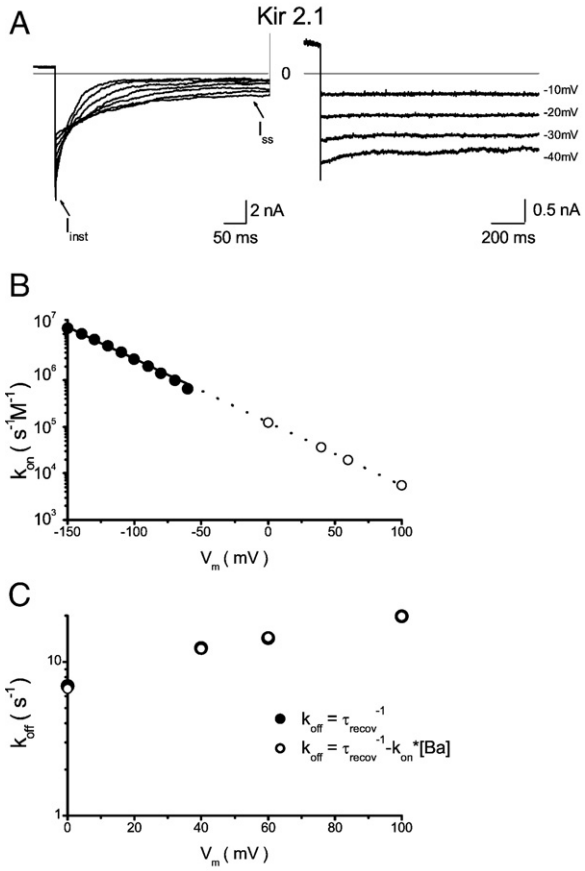

Fig. 2. Kinetics of Ba^{2+} block of the Kir2.1 channel. A: Representative currents recorded at V_m range of −150 to −100 mV (left panel) and at more positive V_m as indicated (right panel) from inside-out patches expressing Kir2.1 channels exposed to 3 μM $[Ba^{2+}]_o$. B: V_m-dependence of k_{on} calculated using Eq. (1) (●). The solid line is the fit to the data using the Boltzmann equation: $k_{on} = k_{on}(0) \times \exp(-z\delta FV_m/RT]$ with $k_{on}(0) = 1.26 \times 10^5$ $M^{-1}s^{-1}$ and $\delta = 0.4$. Symbol, ○, represents extrapolated k_{on} at 0, +40, +60, and +100 mV. The dotted line is the extrapolation of the k_{on}–V_m relationship to +100 mV. C: V_m-dependence of k_{off}. Symbol, ●, denotes k_{off} values calculated by using Eq. (1) and ○ denotes k_{off} values estimated as $1/\tau_{recov}$. $n = 5–12$.

inward currents recorded at V_m ranging from −150 to −100 mV (left panel) decreased over time due to Ba^{2+} block. At more positive V_m, 3 μM extracellular [Ba^{2+}] was unable to block currents at V_m>−40 mV (Fig. 2A, right panel). Since steady-state block, f, was very small, k_{on} values could not be accurately estimated by Eq. (2) at V_m>−40 mV and were obtained from extrapolation. Fig. 2B shows the k_{on} estimated by Eq. (2) (●) and the extrapolated k_{on} (○). Fig. 2C shows the k_{off} calculated by using Eq. (1) (●) and by $1/\tau_{recov}$ (○). Because the two sets of data were superimposed, throughout this study k_{off} were determined as $1/\tau_{recov}$.

3. Results

3.1. Different intracellular blockers retard Ba^{2+} exit from the Kir2.1 pore to varying degrees

Spermine and Mg^{2+} completely inhibit K^+ efflux through Kir channels [20–23], but spermine is much more effective than Mg^{2+} in reducing the rate of Ba^{2+} exit [18]. In this study, we first compared the effects of polyamines of various lengths on Ba^{2+} exit from the Kir2.1 channel. To estimate the Ba^{2+} exit rate at V_m≥0 mV, the rate of recovery from Ba^{2+} block was measured using a two-pulse protocol in inside-out patches (Fig. 3A). The channels were blocked over time by 3 μM Ba^{2+} at −120 mV during the first test pulse (averaged time constant of 72.0±1.3 ms; n=16), then a fraction of the channels was allowed to recover from Ba^{2+} block during the application of recovery voltages (V_r) of different durations before application of the second test pulse. Fig. 3B shows current traces recorded using V_r=+40 mV for the Kir2.1 channel perfused intracellularly with control solution (polyamine- and Mg^{2+}-free), 100 μM spermine, 100 μM spermidine, or 300 μM putrescine. The instantaneous currents recorded with the second test pulse increased when the interval between the two test pulses was increased. The intracellular blockers slowed the rate of recovery from Ba^{2+} block by varying degrees, with spermine being the most potent. A long synthetic polyamine, CGC-11179, can protect several amino acids located internal to residue 160 in the Kir6.2 channel (equivalent to D172 in the Kir2.1 channel) from chemical modification [24]. By comparing the ability of CGC-11179 and spermine to protect the channel pore from chemical modification and their lengths, it has been suggested that the head of CGC-11179 may bind deep in the selectivity filter of the Kir6.2 channel [24]. If this is true, CGC-11179 may displace Ba^{2+} in a way similar to K^+. We therefore examined the effects of CGC-11179 on recovery from Ba^{2+}

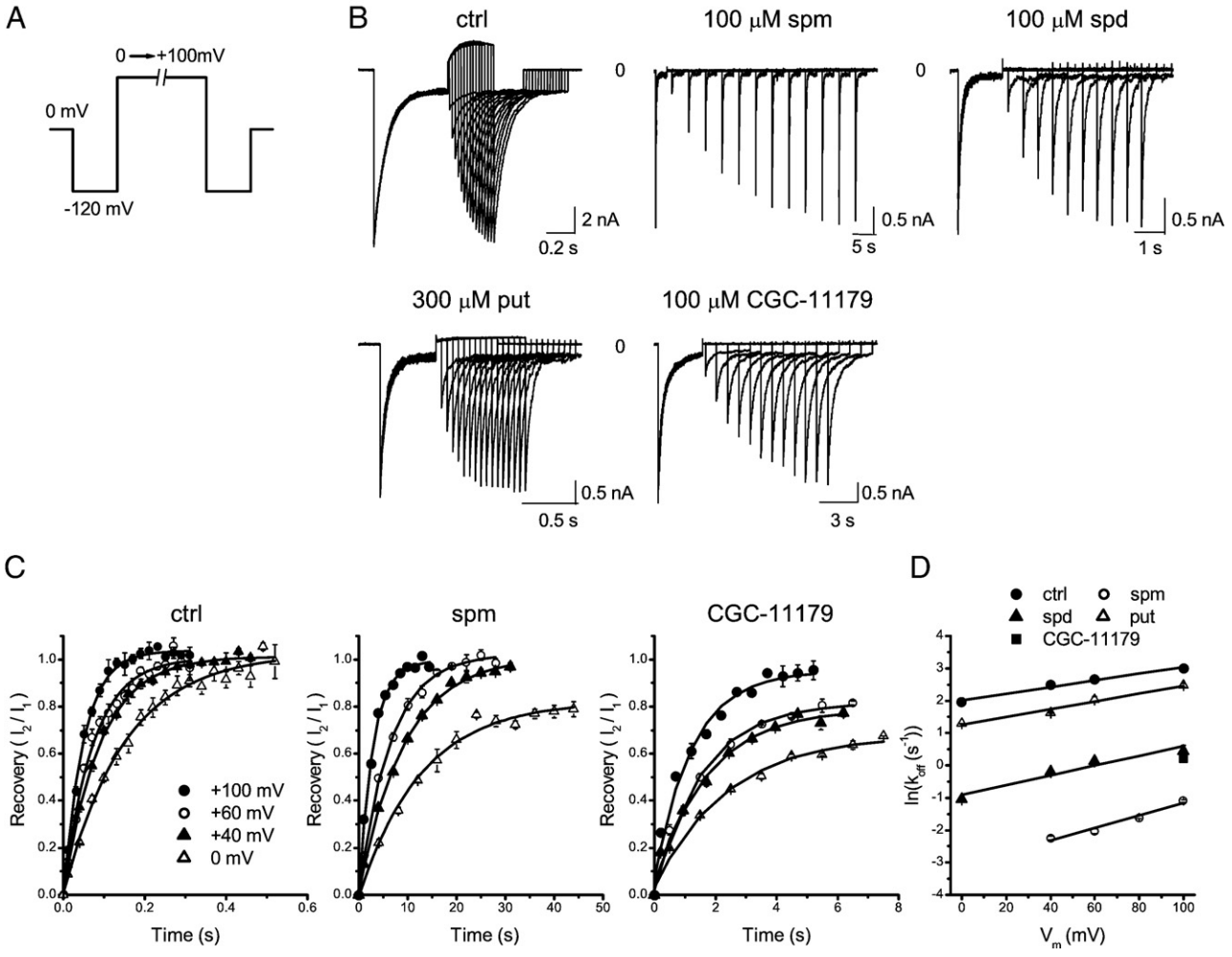

Fig. 3. Effects of different intracellular blockers on recovery from Ba^{2+} block. A: A two-pulse voltage protocol was used to measure recovery from Ba^{2+} block. The time between the two identical test pulses to −120 mV was increased until recovery from Ba^{2+} block reached a steady state. The V_r ranged from 0 to +100 mV. The protocol was applied at 0.02 to 1 Hz. In patches in which Ba^{2+} exit was very slow, the blockers were washed out and the patches held at +40 mV between episodes to ensure complete Ba^{2+} recovery before the subsequent episode. B: Current traces recorded with V_r=+40 mV in the Kir2.1 channel in the presence of control solution or the indicated blocker. C: Time-courses of recovery from Ba^{2+} block at various V_r in control solution, 100 μM spermine, or 100 μM CGC-11179. The recovery was calculated by dividing the (peak current−steady-state current) obtained at the second pulse (I_2) by that at the first pulse (I_1). The solid lines are the fit to the data using a monoexponential function. D: The V_m-dependence of the k_{off} in the presence of various blockers; only the result at V_m=100 mV is shown for CGC-11179. The solid lines are the fit to the data using the Boltzmann equation, $\ln(k_{off})=\ln(k_{off}(0))+z\delta FV_m/RT$, where $k_{off}(0)$ is the k_{off} at 0 mV, z the valence of ions moving during Ba^{2+} exit, δ the apparent electrical distance between the Ba^{2+} binding site and the outer pore of the channel, and F, R, T, and V_m have their usual meanings. $z\delta$ and $k_{off}(0)$ (s^{-1}) were 0.26 and 7.48 in the control (ctrl), 0.49 and 0.04 in spermine (spm), 0.4 and 0.38 in spermidine (spd), and 0.31 and 3.49 in putrescine (put). n=3–8.

block. Fig. 3B shows that CGC-11179 also slowed recovery from Ba^{2+} block, but its effect was less than that of spermine. Fig. 3C shows the time-courses of the averaged fractional recovery from patches exposed to control solution, spermine, or CGC-11179 at different V_r. The recovery time-courses fit an exponential function and the recovery rate ($1/\tau_{recov}$) increased with the V_r. Note that recovery from Ba^{2+} block was not complete when the channels were held at V_r=0 mV in the presence of spermine and at V_r=0 to +60 mV in the presence of CGC-11179. The reason for the incomplete Ba^{2+} recovery is unknown, but could be due to the trapping of Ba^{2+} in the channel or an increase in the Ba^{2+} binding rate in the presence of intracellular blockers. In this study, only time-courses showing complete recovery were used to calculate the Ba^{2+} exit rate, k_{off}. Fig. 3D shows the V_m-dependence of the k_{off} in the presence of control solution or different intracellular blockers. Under all conditions, the k_{off} increased with an increase in the V_r. The k_{off} values in the presence of the blockers were smaller than in the control and the order of the retarding effect of the blockers on Ba^{2+} exit was spermine>CGC-11179≈spermidine>putrescine. The effects of the blockers on k_{off} values indicate that the K^+-Ba^{2+} interaction is critical for Ba^{2+} exit. When this interaction was prevented by the blockers, Ba^{2+} exit was slowed down.

3.2. Competitive effects of K^+ and spermidine on Ba^{2+} exit reveal that at least three K^+ must bind in the inner vestibule to facilitate Ba^{2+} exit

It has been suggested that intracellular K^+ affect the degree of inward rectification by competing with polyamines for the same binding sites [25], so the different effects of blockers on Ba^{2+} exit may be due to different extents of competition between K^+ and blockers. We therefore examined the effect of $[K^+]_i$ on Ba^{2+} exit in the presence or absence of polyamines. Fig. 4A shows traces of currents recorded using the same V_m protocol described in Fig. 3A at $[K^+]_i$ of 20 and 600 mM and a constant extracellular $[K^+]$ of 100 mM (upper panels) and the time-course of recovery from Ba^{2+} block at V_r=+60 mV (lower panels). The recovery was faster at 600 mM $[K^+]_i$ than at 20 mM $[K^+]_i$. Fig. 4B shows that Ba^{2+} exit increased as $[K^+]_i$ increased and did not saturate at a $[K^+]_i$ up to at least 600 mM. Because the V_r was maintained at +60 mV at all $[K^+]_i$, these effects were probably due to a higher driving force at a higher $[K^+]_i$. When $V_r - E_{rev}$ was set at +100 mV, $[K^+]_i$ ranging from 20 to 600 mM had a similar effect on Ba^{2+} exit (Fig. 4C). A further decrease in $[K^+]_i$ to 4 mM resulted in a slight increase in the k_{off}; however, because the ionic strength was so low, the effect of such a low $[K^+]_i$ on Ba^{2+} exit may not be due to the change in $[K^+]_i$ alone. The Kir2.1 channel quickly ran down at a low $[K^+]_i$ and we could not carry out experiments at a $[K^+]_i$<4 mM and obtain a complete dose–response curve, so the contribution of K^+ in the inner vestibule to Ba^{2+} exit could not be directly determined.

In the presence of spermidine under the same conditions as above, Ba^{2+} exit became strongly dependent on $[K^+]_i$ in the range of 20 to 600 mM. Fig. 4B shows the effect of $[K^+]_i$ on the Ba^{2+} exit rate determined at V_r=+60 mV in the presence of 1 and 10 μM spermidine. The V_r was set at a constant value to avoid different degrees of K^+-spermidine competition at different V_r. To eliminate different driving force effects, the k_{off} obtained with spermidine (k_{off} (PA)) was divided by that of the control (k_{off} (ctrl)) at each $[K^+]_i$. Fig. 4D shows the $[K^+]_i$-dependence of the effects of spermidine on Ba^{2+} exit. The dose–response curve was shifted to the right when the concentration of spermidine was increased from 1 to 10 μM due to stronger competition by the blocker with K^+ for binding sites. The Hill coefficient of the dose–response curves in 1 or 10 μM spermidine was 2.4, suggesting that Ba^{2+} exit is facilitated by the cooperative interaction of at least three K^+.

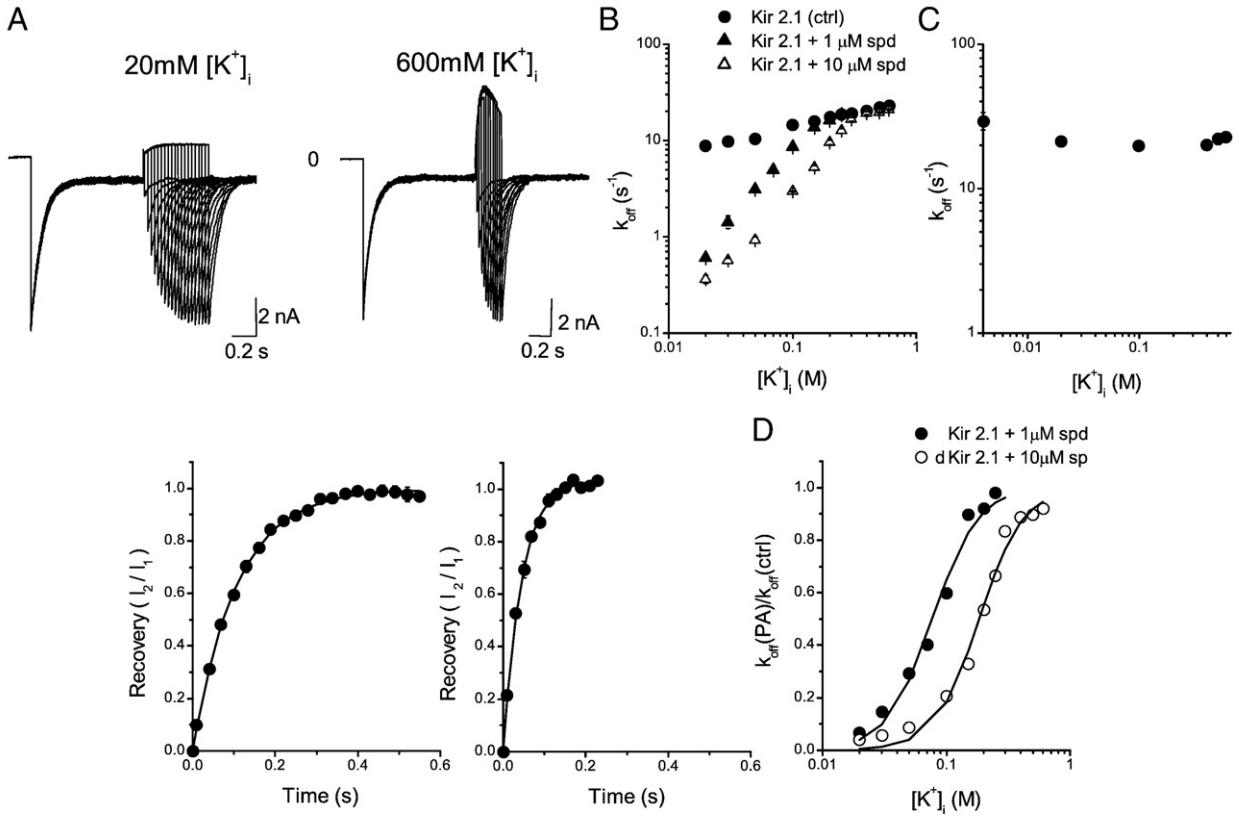

Fig. 4. Effects of $[K^+]_i$ on Ba^{2+} exit. A: Current traces and time-courses of recovery from 3 μM Ba^{2+} block recorded at 20 and 600 mM $[K^+]_i$, respectively. The holding and test potentials were +40 and −80 mV in patches exposed to 20 mM $[K^+]_i$ and −45 and −165 mV at 600 mM $[K^+]_i$. The V_r was +60 mV at both 20 and 600 mM $[K^+]_i$. B: Effects of $[K^+]_i$ on the k_{off} when the V_r was kept at +60 mV for all $[K^+]_i$ in the absence and presence of 1 and 10 μM spermidine. C: The k_{off} values obtained with $V_r - E_{rev}$ = +100 mV in control medium. D: Effects of $[K^+]_i$ on normalized Ba^{2+} exit in the presence of intracellular 1 and 10 μM spermidine at V_r=+60. The smooth curves are the fit of the data to the Hill equation $[1+(K_{0.5}/[K^+]_i)^h]$, where $K_{0.5}$ is the half saturating concentration and h the Hill coefficient. The $K_{0.5}$ and h were respectively 80 mM and 2.37 in 1 μM spermidine and 180 mM and 2.43 in 10 μM spermidine.

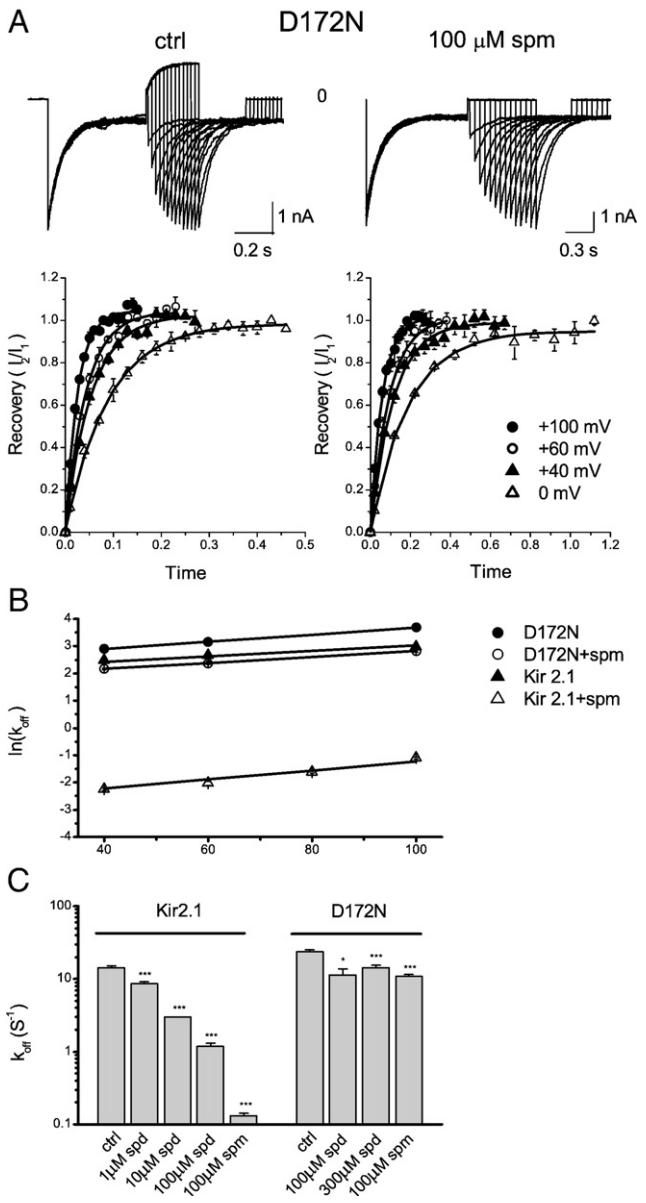

Fig. 5. Effects of spermine on Ba^{2+} exit in the D172N mutant. A: The upper panels show current traces recorded with V_r=+60 mV in the D172N mutant in control solution and 100 μM spermine. The D172N mutant was exposed to 3 μM extracellular Ba^{2+}. The lower panels show time-courses for the recovery from Ba^{2+} block at various V_r in control solution and in spermine. The solid lines are the fit to the data using a monoexponential function. B: V_m-dependence of the k_{off} in control medium and 100 μM spermine. The solid lines are the fit to the data from +40 to +100 mV, using the Boltzmann equation. In the D172N mutant, $z\delta$=0.34 and k_{off} (0)=10.5 s^{-1} in control medium and 0.28 and 5.6 s^{-1} in spermine. Data for the wild-type channel (plotted in Fig. 2D) are shown for comparison. C: Averaged k_{off} in the absence and presence of polyamines for the wild type channel and the D172N mutant. n=3–6. *, p<0.05; ***, p<0.005.

3.3. The effect of polyamines on Ba^{2+} exit is altered by D172N mutation in the water cavity and by M301A mutation in the G-loop

Previous studies show that polyamines inhibit outward currents by interacting with D172 in the water cavity and with E224 and E299 located in the cytoplasmic pore in the Kir2.1 channel [26,27]. Our previous study shows that polyamines interacting with D172 block the Kir2.1 channel pore, whereas polyamines interacting with E224 and E299 do not occlude the large cytoplasmic pore but reduce the diffusion rate of K^+ moving through the cytoplasmic pore via an electrostatics effect [28,29]. To study the effect of K^+-polyamine competition for binding in the water cavity on Ba^{2+} exit, we examined Ba^{2+} ext in the D172N mutant. Fig. 5A shows the currents and recovery time-courses of Ba^{2+} block in the D172N mutant. Compared to the wild-type Kir2.1 channel, Ba^{2+} exit in the absence of intracellular blockers was faster in the D172N mutant. Spermine (100 μM), completely inhibiting outward currents, only slightly decreased the k_{off} at V_r ranging from 0 to +100 mV (Fig. 5B), in contrast to its strong retarding effect on Ba^{2+} exit in the wild type. Fig. 5C shows that, for the wild type channel, increasing spermidine concentrations reduced Ba^{2+} exit in a dose-dependent way and that spermine (100 μM) was more effective than spermidine (10–300 μM). The effects are consistent with K^+ competing with polyamines for binding sites, as shown in Fig. 4D. However, these effects were not observed in the D172N mutant (Fig. 5C), suggesting that the K^+ binding sites involved in facilitating Ba^{2+} exit were not affected by polyamines interacting with E224 and E299 in the mutant. The results show that site D172 is the K^+-polyamine competition site for the regulation of Ba^{2+} exit. Furthermore, the reduced effect of spermine on Ba^{2+} exit in the D172N mutant suggests that the K^+ binding sites involved in facilitating Ba^{2+} exit are located external to sites E224 and E299 in the cytoplasmic pore, i.e. the G-loop and water cavity. We next tested the effects of site-directed mutations in the G-loop on Ba^{2+} exit using mutants M301A, M301G, and A306G.

Fig. 6A shows the currents and recovery time-courses from Ba^{2+} block in the M301A mutant. In the absence of intracellular blockers,

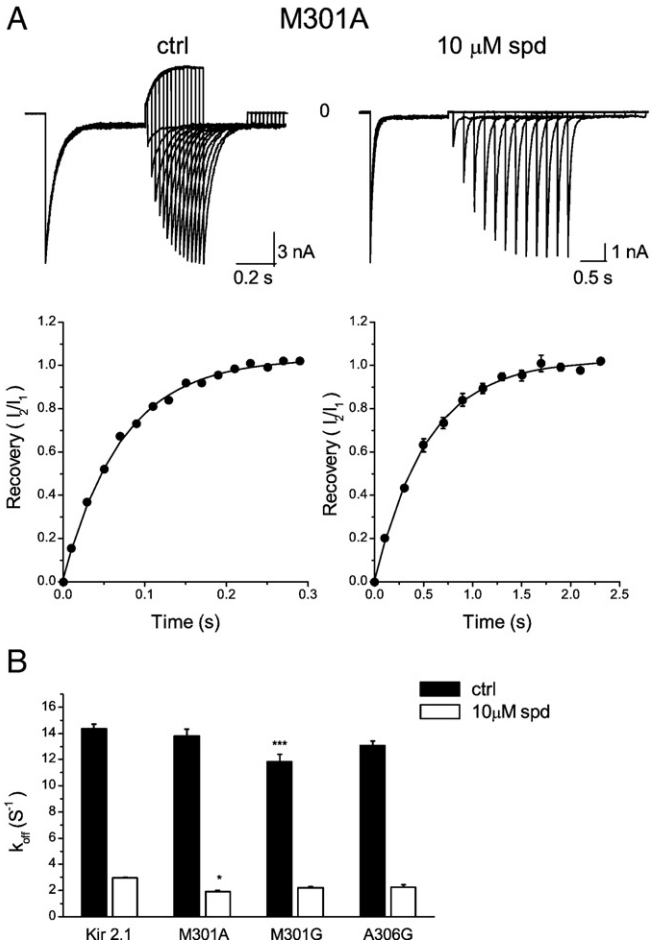

Fig. 6. Effects of 10 μM spermidine on Ba^{2+} exit for the M301A, M301G, and A306G mutants. A: The upper panels show current traces recorded at V_r=+60 mV in control solution and 10 μM spermidine for the M301A mutant. The lower panels show time-courses for the recovery from Ba^{2+} block in control solution and spermidine. The solid lines are the fit to the data using a monoexponential function. B: Averaged k_{off} in the absence and presence of 10 μM spermidine for the wild type channel and the three mutants. n=3–11. *, p<0.05; ***, p<0.005.

the Ba^{2+} exit rate was the same in the M301A mutant and the wild type. The effect of 10 μM spermidine on Ba^{2+} exit was slightly greater in the M301A mutant than in the wild type (Fig. 6B). In the M301G mutant, the Ba^{2+} exit rate was slower in control medium than in the wild type, but the effect of 10 μM spermidine on Ba^{2+} exit was the same in both (Fig. 6B). These results suggest that K^+ bound at or near site M301 in the G-loop may be involved in K^+ interaction that regulates Ba^{2+} exit. Ba^{2+} exit rates were the same in the A306G mutant and wild type channel in both control medium and 10 μM spermidine (Fig. 6B). Because only the glycine substitution was well tolerated at site 306 [10], the effects of other mutations at site 306 were not examined. Whether both sites in the G-loop can be simultaneously occupied by two K^+ or whether both are involved in facilitating Ba^{2+} exit requires further investigation.

4. Discussion

K^+ binding and concerted K^+ transport in the selectivity filter contribute to the near-diffusion limit conductance of K^+ channels [6,9,30], but these properties in the inner vestibule of K^+ channels are not well studied. The previous study of crystallized Kir3.1–KirBac1.3 channels shows one K^+ binding site in the water cavity and two sites at the inner helix bundle gate and the apex of the inner vestibule formed by the G-loop [7], but their contribution to permeation has not been studied. For example, it is unknown whether all three binding sites are occupied during ion conduction. It has been shown that the selectivity filter has four K^+ binding sites in the crystallized KcsA channel [5] but only two K^+ are simultaneously occupying the selectivity filter when the channel is conducting ions [31]. It is difficult to study ion permeation because ion conduction rate is very fast in ion channels. Using a novel experimental design, we determine the role in permeation of K^+ in the inner vestibule. We find that at least three K^+, interacting with positive cooperativity, are involved in Ba^{2+} exit and that the K^+ binding sites are located between the cytoplasmic pore and selectivity filter. In addition, the results suggest that K^+ bound at or near site D172 and in G-loop are involved in facilitating Ba^{2+} exit into the extracellular pore.

Another interesting finding of this study is that polyamines do not mimic the effects of K^+ in accelerating Ba^{2+} exit from the pore. Instead, polyamines, including a long synthetic polyamine, CGC-11179, slow down Ba^{2+} exit. Intracellular polyamines are known to block the Kir2.1 channel but the physical location of polyamine binding remains unclear. Some studies propose a shallow model of spermine block with spermine binding between the D172 site and several rings of negatively charged residues located in the cytoplasmic pore in the Kir2.1 channel [32,33]. Other studies suggest a deep model of polyamine block with spermine binding between the aspartate residue in the water cavity and the selectivity filter in Kir2.1 and Kir6.2 channels [28,34,35]. However, it remains unknown how “deep” the polyamine is located in the pore. For example, it is unclear whether polyamines can insert in the selectivity filter. By examining the effects of polyamine occupancy on the rate of MTSEA modification of cysteine residues located at pore-lining sites in Kir6.2[N160D] channels, Kurata et al. [34,36] suggest that the leading amine of spermine and CGC-11179 can be approaching or enter the selectivity filter. The conclusion is reached based on the assumption that polyamines do not bend or tilt in the large water cavity. Our data show that polyamines reduce Ba^{2+} exit into the extracellular space, suggesting that polyamines may not replace Ba^{2+} from its binding site at T141. However, we cannot rule out other possibilities such as a polyamine inserting in the selectivity filter and also induce conformational changes of the selectivity filter such that Ba^{2+} exit rate is reduced.

Fig. 4D suggests that the cooperative interaction of K^+ is important for facilitating Ba^{2+} exit. However, in addition to K^+ binding, other mechanisms may be involved in the facilitating effects of $[K^+]_i$ on Ba^{2+} exit. It is possible that Ba^{2+} exit requires further K^+-Ba^{2+} interactions, e.g. the movement of a K^+ from the water cavity to the innermost K^+ binding site (S4) in the selectivity filter may displace Ba^{2+} from its binding site and facilitate Ba^{2+} exit by repulsion. Recently, the concerted transport of K^+ in the selectivity filter has been modeled using molecular dynamics simulations [30]. Based on the analysis of the interaction energies, it is suggested that the concerted movement is dominated by shorter-range dipolar interactions involving the ion, water, and carbonyl groups, rather than by long-range electrostatic ion–ion repulsion. It is possible that K^+ entry into the S4 site may be increased by K^+–K^+ interaction and/or concerted K^+ transport in the G-loop and water cavity. For example, since some water molecules may separate the K^+ in the cavity and the Ba^{2+} ion in the S4 site, these have to move to allow the K^+ to move to S4 to displace Ba^{2+}. In addition, because the electron density map of the crystal structure of the KcsA channel shows a focused position for the K^+ in the water cavity [5], K^+ may move from the G-loop through the water cavity into the selectivity filter by a specific route determined by the K^+ channel and K^+–water movements. In summary, K^+ may interact with one another and with the channel pore in order to flow through the channel, instead of just binding and passively diffusing in the inner vestibule of the Kir2.1 channel.

Inward rectification is weaker in the D172N mutant than in the wild-type Kir2.1 channel [22,26,37]. In addition, molecular calculations suggest that a negatively-charged residue in the water cavity may stabilize the binding of K^+ in the water cavity and thus decrease the rate of K^+ entry into the selectivity filter of the Kir3.2 channel [38]. Therefore, it is likely that the K^+–Ba^{2+} interaction is stronger, and that K^+ can compete more efficiently with polyamines for binding sites, in the D172N mutant than in the wild-type Kir2.1 channel. Indeed, in control medium, the Ba^{2+} exit rate was faster for the D172N mutant than the wild type and spermine did not efficiently reduce Ba^{2+} exit in the D172N mutant (Fig. 5). It has been shown that inward rectification is weaker in the M301A mutant than in the wild type [10], suggesting that K^+ compete more efficiently with polyamines for binding sites in this mutant. However, 10 μM spermidine was more effective in slowing Ba^{2+} exit in the M301A mutant than in the wild type (Fig. 6). These results suggest that K^+, polyamines, and Ba^{2+} interact in a complex manner that is not yet completely understood.

In conclusion, we showed that the binding of K^+ in the water cavity and maybe in the G-loop is critical in facilitating Ba^{2+} exit from the selectivity filter. We provide functional evidence for the three K^+ binding sites in the inner vestibule previously identified by crystal structure study [7]. This study examines the functional roles of K^+ in the G-loop and water cavity of the Kir2.1 channel. Further investigations are required to understand the complex interaction of ions with the channel pore.

Acknowledgements

We thank Dr. Lily Jan for kindly providing the Kir2.1 clone. We are grateful to Dr. Tom Barkas for English editing. This work was supported by the Academia Sinica and by the National Science Council of Taiwan (grant 96-2320-B001-002).

References

[1] B. Hille, W. Schwarz, Potassium channels as multi-ion single-file pores, J. Gen. Physiol. 72 (1978) 409–442.
[2] J. Neyton, C. Miller, Discrete Ba^{2+} block as a probe of ion occupancy and pore structure in the high-conductance Ca^{2+}-activated K^+ channel, J. Gen. Physiol. 92 (1988) 569–586.
[3] B. Vestergaard-Bogind, P. Stampe, P. Christophersen, Single-file diffusion through the Ca^{2+}-activated K^+ channel of human red cells, J. Membr. Biol. 88 (1985) 67–75.
[4] A.L. Hodgkin, R.D. Keynes, The potassium permeability of a giant nerve fibre, J. Physiol. 128 (1955) 61–88.
[5] D.A. Doyle, C.J. Morais, R.A. Pfuetzner, A. Kuo, J.M. Gulbis, S.L. Cohen, B.T. Chait, R. MacKinnon, The structure of the potassium channel: molecular basis of K^+ conduction and selectivity, Science 280 (1998) 69–77.
[6] Y. Zhou, J.H. Morais-Cabral, A. Kaufman, R. MacKinnon, Chemistry of ion coordination and hydration revealed by a K^+ channel-Fab complex at 2.0 Å resolution, Nature 414 (2001) 43–48.

[7] M. Nishida, M. Cadene, B.T. Chait, R. MacKinnon, Crystal structure of a Kir3.1-prokaryotic Kir channel chimera, EMBO J. 26 (2007) 4005–4015.
[8] Y. Zhou, R. MacKinnon, The occupancy of ions in the K^+ selectivity filter: charge balance and coupling of ion binding to a protein conformational change underlie high conduction rates, J. Mol. Biol. 333 (2003) 965–975.
[9] S. Berneche, B. Roux, Energetics of ion conduction through the K^+ channel, Nature 414 (2001) 73–77.
[10] S. Pegan, C. Arrabit, W. Zhou, W. Kwiatkowski, A. Collins, P.A. Slesinger, S. Choe, Cytoplasmic domain structures of Kir2.1 and Kir3.1 show sites for modulating gating and rectification, Nat. Neurosci. 8 (2005) 279–287.
[11] M. Nishida, R. MacKinnon, Structural basis of inward rectification: cytoplasmic pore of the G protein-gated inward rectifier GIRK1 at 1.8 Å resolution, Cell 111 (2002) 957–965.
[12] J. Neyton, C. Miller, Potassium blocks barium permeation through a calcium-activated potassium channel, J. Gen. Physiol. 92 (1988) 549–567.
[13] H. Zhou, S. Chepilko, W. Schutt, H. Choe, L.G. Palmer, H. Sackin, Mutations in the pore region of ROMK1 enhance Ba block, Am. J. Physiol. Cell Physiol. 291 (1996) 1949–1956.
[14] Y. Jiang, R. MacKinnon, The barium site in a potassium channel by X-ray crystallography, J. Gen. Physiol. 115 (2000) 269–272.
[15] O.P. Hamill, A. Marty, E. Heher, B. Sakmann, F.J. Sigworth, Improved patch-clamp techniques for high-resolution current recording from cells and cell-free membrane patches, Pflugers Arch. Eur. J. Physiol. 391 (1981) 85–100.
[16] D.W. Hilgemann, The giant membrane patch, In: B. Sakmann, E. Neher (Eds.), Single-Channel Recording, Plenum Press, New York, 1995, pp. 307–328.
[17] A.E. Martell, R.M. Smith, Critical Stability Constants, Plenum Press, New York, 1974.
[18] R.-C. Shieh, J.-C. Chang, J. Arreola, Interaction of Ba^{2+} with the pores of the cloned inward rectifier K^+ channels Kir2.1 expressed in *Xenopus* oocytes, Biophys. J. 75 (1998) 2313–2322.
[19] M. Holmgren, P.L. Smith, G. Yellen, Trapping of organic blockers by closing of voltage-dependent K^+ channels: evidence for a trap door mechanism of activation gating, J. Gen. Physiol. 109 (1997) 527–535.
[20] H. Matsuda, A. Saigusa, H. Irisawa, Ohmic conductance through the inwardly rectifying K channel and blocking by internal Mg^{2+}, Nature 325 (1987) 156–159.
[21] C. Vandenberg, Inward rectification of a potassium channel in cardiac ventricular cells depends of internal magnesium ions, Proc. Natl. Acad. Sci. U. S. A. 84 (1987) 2560–2564.
[22] E. Ficker, M. Taglialatela, B.A. Wible, C.M. Henley, A.M. Brown, Spermine and spermidine as gating molecules for inward rectifier K^+ channels, Science 266 (1994) 1068–1072.
[23] A.N. Lopatin, E.N. Makhina, C.G. Nichols, Potassium channel block by cytoplasmic polyamines as the mechanism of intrinsic rectification, Nature 372 (1994) 366–369.
[24] H.T. Kurata, L.J. Marton, C.G. Nichols, The polyamine binding site in inward rectifier K^+ channels, J. Gen. Physiol. 127 (2006) 467–480.
[25] A.N. Lopatin, C.G. Nichols, [K^+] dependence of polyamine-induced rectification in inward rectifier potassium channels (IRK1, Kir2.1), J. Gen. Physiol. 108 (1996) 105–113.
[26] J. Yang, Y.N. Jan, L.Y. Jan, Control of rectification and permeation by residues in two distinct domains in an inward rectifier K^+ channel, Neuron 14 (1995) 1047–1054.
[27] Y. Kubo, Y. Murata, Control of rectification and permeation by two distinct sites after the second transmembrane region in Kir2.1 K^+ channel, J. Physiol. 531 (2001) 645–660.
[28] H.K. Chang, R.C. Shieh, Conformational changes in Kir2.1 channels during NH_4^+-induced inactivation, J. Biol. Chem. 278 (2003) 908–918.
[29] S.H. Yeh, H.K. Chang, R.C. Shieh, Electrostatics in the cytoplasmic pore produce intrinsic inward rectification in Kir2.1 channels, J. Gen. Physiol. 126 (2005) 551–562.
[30] J.F. Gwan, A. Baumgaertner, Cooperative transport in a potassium ion channel, J. Chem. Phys. 127 (2007) 045103.
[31] J.H. Morais-Cabral, Y. Zhou, R. MacKinnon, Energetic optimization of ion conduction rate by the K^+ selectivity filter, Nature 414 (2001) 37.
[32] D. Guo, Z. Lu, Interaction mechanisms between polyamines and IRK1 inward rectifier K^+ channels, J. Gen. Physiol. 122 (2003) 485–500.
[33] D. Guo, Y. Ramu, A.M. Klem, Z. Lu, Mechanism of rectification in inward-rectifier K^+ channels, J. Gen. Physiol. 121 (2003) 261–275.
[34] H.T. Kurata, L.R. Phillips, T. Rose, G. Loussouarn, S. Herlitze, H. Fritzenschaft, D. Enkvetchakul, C.G. Nichols, T. Baukrowitz, Molecular basis of inward rectification: polyamine interaction sites located by combined channel and ligand mutagenesis, J. Gen. Physiol. 124 (2004) 541–554.
[35] S.A. John, L.H. Xie, J.N. Weiss, Mechanism of inward rectification in Kir channels, J. Gen. Physiol. 123 (2004) 623–625.
[36] H.T. Kurata, K. Diraviyam, L.J. Marton, C.G. Nichols, Blocker protection by short spermine analogs: refined mapping of the spermine binding site in a Kir channel, Biophys. J. 95 (2008) 3827–3839.
[37] P. Stanfield, N. Davies, P. Shelton, M. Sutcliffe, I. Khan, W. Brammar, E. Conley, A single aspartate residue is involved in both intrinsic gating and blockage by Mg^{2+} of the inward resctifier, IRK1, J. Physiol. 478 (1994) 1–6.
[38] D. Bichet, M. Grabe, Y.N. Jan, L.Y. Jan, Electrostatic interactions in the channel cavity as an important determinant of potassium channel selectivity, Proc. Natl. Acad. Sci. U. S. A 103 (2006) 14355–14360.